



**READ 2024**  
RESEARCH & EDUCATION IN AIRCRAFT DESIGN  
WARSAW, POLAND | 6-8 NOVEMBER 2024



## OPTICAL MEASUREMENT SYSTEM SUPPORTING THE NAVIGATION OF RAPIDLY ROTATING OBJECTS

Dawid Florczak<sup>1</sup>, Gustaw Mazurek<sup>2</sup> & Robert Głębocki<sup>3</sup>

<sup>1</sup>Institute of Aeronautics and Applied Mechanics, Warsaw University of Technology, e-mail: dawid.florczak@pw.edu.pl

<sup>2</sup>Institute of Electronic Systems, Warsaw University of Technology, e-mail: gustaw.mazurek@pw.edu.pl

<sup>3</sup>Institute of Aeronautics and Applied Mechanics, Warsaw University of Technology, e-mail: robert.glebocki@pw.edu.pl

### Abstract

The primary challenge in navigating rotating objects using inertial navigation systems (INS) with MEMS sensors is accurately determining their rotational speed. The limitations in precisely measuring this speed are the main sources of errors in inertial navigation. These inaccuracies present a significant obstacle to enhancing and controlling traditional, unguided rotating object designs. To address this, an innovative system has been proposed to support the navigation of rapidly rotating objects by predicting navigation data through algorithms that analyze changes in environmental conditions during movement in space.

This work delves into a designed system that fundamentally assumes the development of a low-cost measurement framework using various sensors to record different types of electromagnetic radiation (visible light, infrared, ultraviolet light). The estimation of navigation data in the rotational channel will be carried out using algorithms that calculate the time between the recorded maximum and minimum values of the aforementioned types of radiation.

To investigate the essence of the phenomenon, a dedicated research station was developed, allowing for experiments within the angular velocity range of 0 - 5400 %/sec, with the capability of altering the angle of attack between 0-50 °.

The data obtained will facilitate the key stage of research: the development of various algorithms tailored to different atmospheric phenomena such as fog, heavy cloud cover, strong sunlight, and varying conditions of day and night. Ultimately, it is anticipated that the most optimal algorithm for specific system conditions will be selected based on lighting and time-of-day conditions.

**Keywords:** fast rotating objects, navigation without GNSS, light sensors, Infrared sensors

### 1. Introduction

Due to the rapid advancement of microelectromechanical systems (MEMS) and their numerous advantages, such as miniaturization, low cost, low power consumption, and environmental resistance, there is currently a high frequency of use of MEMS-based inertial navigation systems in most modern flying objects [1]. Broadly speaking, the case of inertial navigation is a particular instance of a system highly susceptible to drift and gyroscope saturation. Moreover, the dynamics of fast-spinning objects and the complexity of acquiring gyroscopes with appropriate angular registration ranges and resolution is a highly intricate concept [2].

#### 1.1 Current state of knowledge

Specifically, the commercial market offers gyroscope systems capable of registering angular velocities of up to 20,000 %/sec. However, these systems are characterized by low sensitivity and significant temperature-induced variations in gain and offsets. An example of this is the MEMS gyroscope from Analog Devices, model ADXRS649BBGZ, which has the capability to register high angular velocities at  $\pm 20,000$  %/sec. Yet, with a sensitivity of only 0.1 mV/deg/s, a substantial temperature impact of  $\pm 2$  percent, and low data registration resolution, this sensor is not suitable for use in precise navigation

systems. Additionally, even for lower angular velocity ranges around 4000 %/sec, the available sensors on the market are inadequate for precise navigation applications. For instance, the ASM330LHBTR sensor, despite its high sensitivity of 0.064 mg/LSB, lacks sufficient resolution (only 16-bit) and is significantly affected by temperature changes [3]. The view of the ADXRS649BBGZ sensor and the ASM330LHBTR sensor is shown in Figure 1.



Figure 1 – ADX RS649BBGZ (left) and ASM330 LHBT sensor (right).

An analysis of sensors, based on available gyroscope distribution platforms (such as Farnell, Mouser, TME, DigiKey), revealed that only sensors with a resolution range of 2000 %/sec possess the necessary parameters to build a precise navigation system. Moreover, even the use of highly precise gyroscopes with appropriate parameters is plagued by various errors, often increasing over time, such as gyroscopic drift due to the physics of their operation. Gyroscopic drift in an inertial navigation system, without support from other navigation systems, can lead to a loss of precision in even the best gyroscopes over time. In essence, disturbances in the process of delivering navigational information, particularly in the determination of angular velocities, also result in a drastic decline in the quality of navigational data across other motion channels of the object. A notable example of this is the challenge of correctly determining the direction of gravitational force in the absence of accurate rotational data, where even the simple task of determining the direction of Earth's gravity vector becomes a significant challenge for inertial systems [4].

The issue of gyroscope saturation is often addressed by various companies and research institutions through the use of accelerometers positioned away from the object's rotation axis. However, the phenomenon of calculating rotational speeds using accelerometers placed at specific distances from the rotation axis, due to their even greater sensitivity to temperature changes compared to gyroscopes, has not yet been confirmed. A clear example of this is the fact that no precise navigation system has been developed that significantly utilizes this phenomenon [5]. Additionally, it is important to note that the use of multiple accelerometers positioned at varying distances from the rotation axis requires the application of advanced mathematical models for estimating navigational data in the rotation channel, including multi-sensor data fusion models, which have high computational power requirements. The necessity of using high-performance microprocessors and implementing advanced mathematical models in the form of highly efficient low-level code entails several challenges, such as high production and design costs of the navigation system itself [6].

For the effective use of inertial navigation systems, the implementation of additional calibration systems is essential to maintain the assumed quality of navigational data over time [7].

## 2. Characteristics of the problem

Limited angular velocity measurement ranges and time-accumulating errors (gyroscopic drift) are critical challenges in the navigation of rapidly spinning objects using MEMS-based systems, stemming from the inherent nature of gyroscopes [8]. It is also important to highlight that issues arising at

high rotational speeds of rapidly spinning objects affect not only gyroscopes but also accelerometers, involving multiple aspects. The key factors contributing to decreased accuracy in spatial orientation determination within inertial navigation units include:

- **Gyroscopic Drift:** Measurements of high angular velocities are susceptible to drift (a slow increase in errors over time), resulting from production imperfections, temperature fluctuations, and mechanical stresses caused by acting forces [9].
- **Centrifugal Effects:** High angular velocities can expose MEMS sensors to centrifugal forces. As a result, the forces generated in the measurement system may deform or stress the sensor elements. Consequently, changes in sensor characteristics may occur, leading to measurement inaccuracies and contributing to overall errors in the inertial navigation system [10].
- **Vibrations and Mechanical Resonance:** The operation of inertial navigation systems within an object exposed to vibrations and mechanical resonances resulting from both translational and rotational motion is also prone to errors due to the nature of movement. High rotational speeds can induce vibrations and mechanical resonances within MEMS sensors, potentially disrupting the operation of accelerometers and gyroscopes, leading to inaccurate readings. Mechanical resonances may cause temporary instability and errors (additional noise) in the sensor's communication lines [11].
- **Limited Dynamic Range:** MEMS sensors often have limitations in their dynamic range (the range of accelerations or angular velocities they can accurately measure). Particularly in rocket technology, a significant issue is acquiring sensors with a measurement range corresponding to the actual rotational velocities possible during an object's motion. Sensors operating at the edge of their measurement range are prone to saturation and accuracy loss. You will receive confirmation message shown on the screen after correct paper addition [12].
- **Cross-Axis Sensitivity:** MEMS sensors may exhibit cross-axis sensitivity, meaning that accelerations or rotations along one axis can significantly influence measurements along other axes. Due to the physics of rapidly spinning objects, it is understood that rotational velocities occur along more than one axis of the body, for example, due to precessional motion. The occurrence of high rotational velocities in such a system can exacerbate cross-axis sensitivity, leading to additional errors in the calculated navigational parameters [13].
- **Environmental Conditions:** The extreme conditions encountered on spinning objects introduce factors that particularly affect the accuracy of inertial navigation systems. Specifically, increased temperature and mechanical stresses, as described above, can further exacerbate sensor drift and cause other errors. It is important to note that the factors affecting the accuracy of MEMS-based inertial navigation are multifaceted. Eliminating one error-inducing factor may not significantly improve the final accuracy of the navigation system. Therefore, a multi-faceted approach to improving measurement system accuracy is essential [14].

To address these challenges, a multi-level approach to improving measurement system accuracy is necessary. To reduce the impact of time-accumulating errors in MEMS-based inertial navigation, calibration techniques are often employed. Another relatively common solution is the use of advanced filtering algorithms and machine learning algorithms to enhance the accuracy and reliability of navigation data. It should also be noted that the popularity of such solutions is currently increasing due to the rapid development of microprocessors and the growth of available computational power. Moreover, combining sensors with other navigation systems, such as satellite navigation systems (e.g., GPS, Beidou, GLONASS, Galileo), is particularly popular. However, due to the ease of disrupting satellite navigation systems, these systems are currently not considered for general applications. A clear example of this is the Russian Murmansk-BN system [15]. The MURMANSK-BN system is one of the most advanced electronic warfare tools used by Russia. Its ability to disrupt GPS signals is of significant strategic and operational importance, particularly in the context of military operations and protecting key areas. The Murmansk-BN has an operational range of up to 5000 km, meaning

it can disrupt GPS signals over vast areas, both on land and at sea. It is equipped with advanced technologies that allow precise disruption of signals on selected frequencies. The Murmansk-BN can emit jamming signals within the frequency range used by GPS satellites, preventing GPS receivers from receiving correct navigational data. Given the above, there is currently a clear need to design an inertial navigation support system that does not rely on navigational data from traditional satellite navigation systems. A view of one of the antennas of the “Murmansk-BN” system is shown in Figure 2.

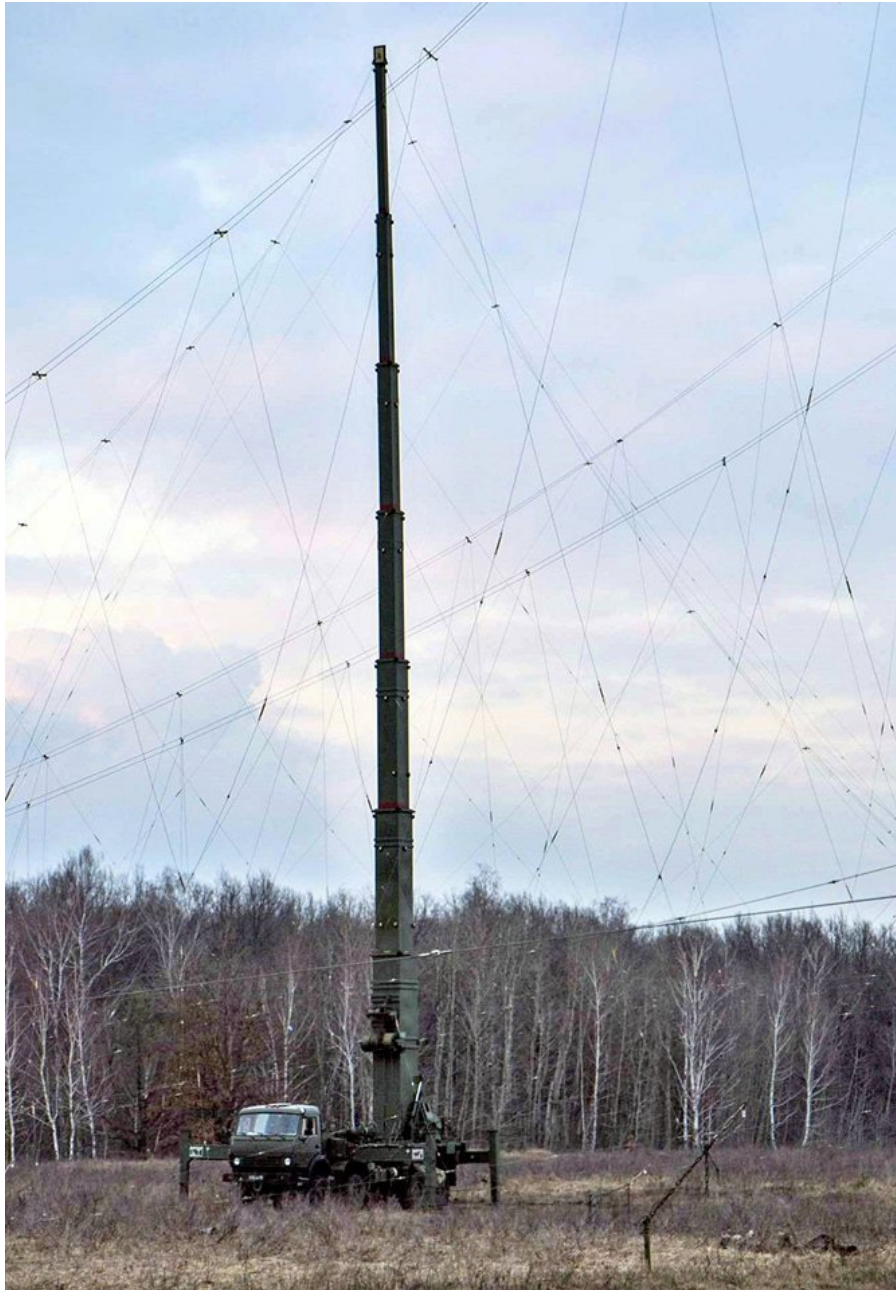


Figure 2 – Long-Range EW System “Murmansk-BN”.

A potential solution to this problem is the development of a dedicated support system for the navigation of rapidly spinning objects, based on the prediction of navigational data through algorithms analyzing environmental changes occurring during spatial motion. The designed system, in its main concept, will rely on a low-cost measurement system utilizing a series of sensors that register various electromagnetic radiation (visible light, infrared, ultraviolet). The estimation of navigational data in the rotational channel will be carried out using algorithms that count the time between the recorded max. and min. values of the mentioned types of radiation. Furthermore, the concept of calibrating the inertial navigation system, even in its most minimalist version, assumes the delivery of naviga-

tional information in the rotational channel after each object rotation, which, considering the values of gyroscopic drift and other parameters of MEMS-based gyroscopes, will not significantly degrade the quality of the provided navigational information. Essentially, the proposed system prototype will significantly improve access to high-precision navigation systems. The measurement system can be easily paired with a commercial inertial navigation unit and will be entirely immune to the factors mentioned above that induce strong errors in inertial navigation.

### 3. Results and discussion

#### 3.1 The main purpose of the work

The objective of the project is to develop an innovative navigation support system for of rapidly spinning objects based on the prediction of navigational data using algorithms that analyze changes in environmental conditions occurring during motion in space. The resulting system will allow for the reduction or complete elimination of certain error components in gyroscopes and accelerometers, which accumulate over time, as well as errors resulting from other operational factors affecting the inertial navigation system used in fast-rotating objects. In particular, it is planned to employ a wide range of sensors registering various electromagnetic waves, starting from infrared waves (ranging from 780 nanometers to 1 millimeter), visible light (wavelengths from 380 to 750 nanometers), ultraviolet radiation in the UV-A range (from 320 to 400 nanometers), and combinations of the aforementioned electromagnetic waves in the form of an integrated single sensor. The estimation of navigational data in the rotation channel will be performed using algorithms that measure the time between the recorded maximum and minimum values of the mentioned types of radiation. The application of data fusion obtained from a set of sensors registering various electromagnetic waves will allow for the complete independence of the inertial navigation systems from satellite navigation systems support. This will enable the system to achieve immunity to intentional and accidental interference and calibration of the inertial navigation system's readings in the rotation channel. Figure 3 below shows the size of the IR sensor, the size of which corresponds to the size of the sensors of the other selected electromagnetic waves.

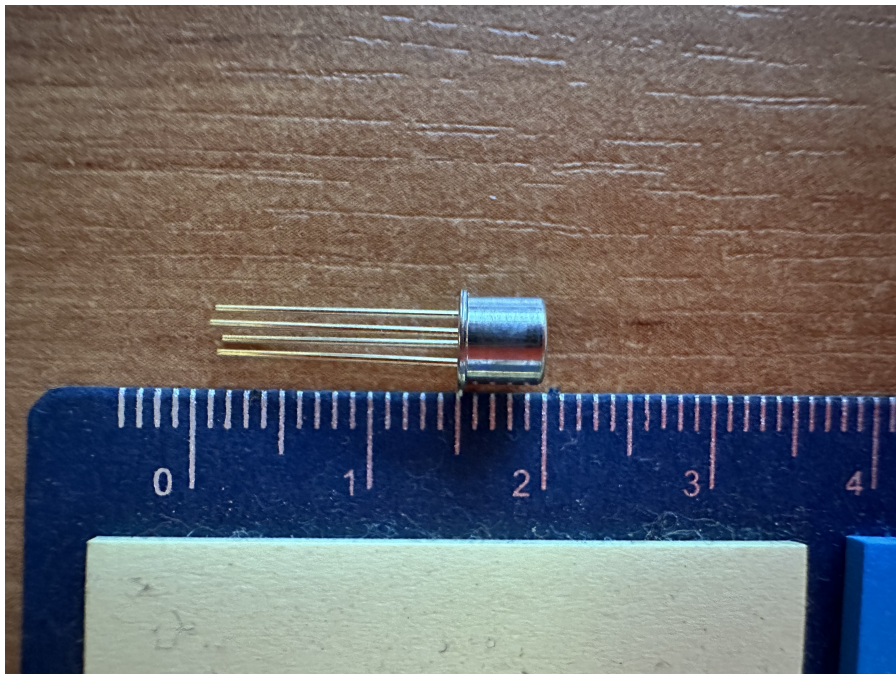


Figure 3 – The size of the sensors of the selected electromagnetic waves.

#### 3.2 Test stand

In order to achieve a properly functioning system as described above, it is necessary to conduct a detailed research and testing process of the developed technology under diverse atmospheric

conditions. For this reason, the development of a dedicated test bench is essential, enabling the simulation of the motion components of a fast-rotating object that determine the data obtained from individual sensors. The planned work includes the development of a test bench with 2 degrees of freedom. Specifically, the test bench will allow for the simulation of rotational motion of the object within a range of  $\pm 5400$  °/sec, with the possibility of adjusting the angle of attack within a range of 0-50°. However, it should be emphasized that the key requirement for investigating the whole essence of the phenomenon was to obtain a range of angular velocities of the order of 0-3600 °/s, which reflect the speeds of rapidly rotating objects developed by the Warsaw University of Technology. It should also be emphasized that in the next stages of the work, tests are planned in real conditions on one of the carriers (fast-spinning objects) which are tested by the Warsaw University of Technology. The final integrated test bench will enable an extensive research campaign that will take into account system operation scenarios under varying atmospheric conditions experienced throughout all seasons in our country. This includes conditions such as cloudy winter days and nights, stormy spring periods, sunny summer days and clear nights, foggy autumn mornings and nights, as well as other typical weather conditions for Central and Eastern Europe. Conducting detailed tests and research under diverse atmospheric conditions will allow for the creation of a dedicated database, which will facilitate the accurate development of algorithms for estimating navigational data, particularly rotational channel navigation data. The view of the designed test stand concept is presented in Figure 4 below.

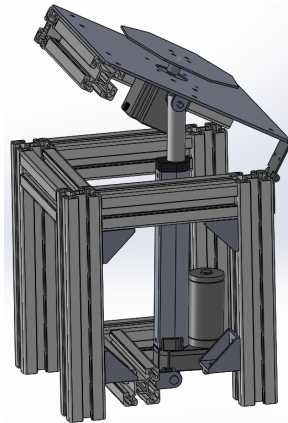


Figure 4 – Test stand concept.

The view of the completed test stand is presented in Figure 5.



Figure 5 – Integrated test stand with recording equipment.

However, it should be emphasized that in addition to the mechanical part of the test stand, it was necessary to develop an integrated controller that would allow for precise control of the stand from a PC. For this purpose, a popular and reliable solution based on the LOGO Siemens controller was selected. In the next step, dedicated control software was implemented, which allows for direct control of the test stand from a computer, both in terms of controlling the test stand to specific research parameters and introducing research scenarios consisting of different angles of attack and different rotational speeds. Figure 6 below shows the appearance of the test stand controller and the view of the source code of the control software, which was created in the Python programming language.

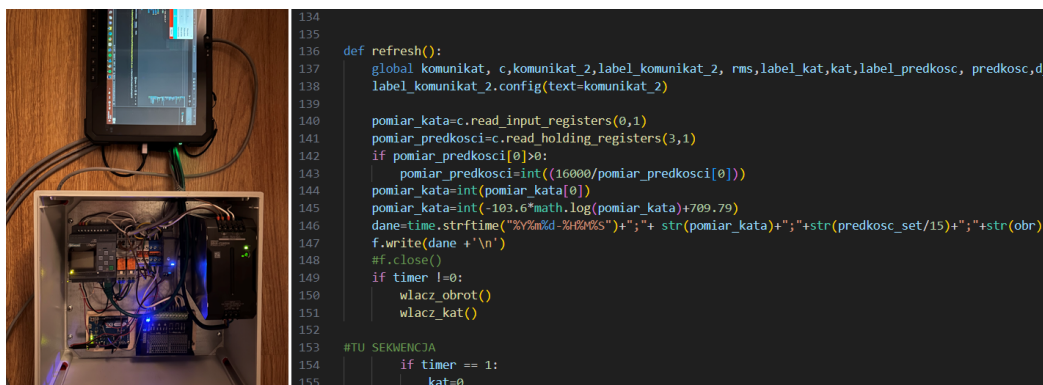


Figure 6 – Control equipment.

Finally, after completing the start-up process of the station, the precision of the generated angular velocity was confirmed at a level of less than 1 percent error, using a Nova-Pro 100 laser tachometer

### 3.3 REClight – Optoelectrical Sensor Data Logger

#### 3.3.1 General structure and functional parameters

The hardware construction of REClight device consists of three main parts, as shown in Fig. 7:

- a set of optoelectrical sensors,
- analog processing board,
- digital processing board.

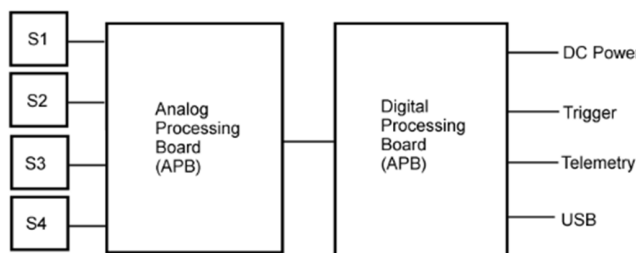


Figure 7 – Simplified block diagram of the REClight device.

There are four optoelectrical sensors connected to the device (S1 . . . S4), each operating in a different spectral range of the light. Three sensors (for visible and UV light) are realized as photodiodes, and one sensor (for IR) is in a form of thermopile. Therefore, IR sensor needs a different analog front-end (AFE) in an input stage of the device, as described in the next Section. The analog and digital functionalities have been physically divided into separate printed circuit boards (PCBs) to reduce a noise level in the analog circuits resulting from the activity of digital parts. Moreover, such an approach allows us to reduce the physical dimensions of PCBs in order to fit into the required space in an experimental scientific rocket. Both PCBs are electrically connected with just one 2x7 pin connector and mechanically – with eight spacer posts. The assembled PCBs are shown separately in Fig. 8, and after mechanical assembling – in Fig. 9 (without the sensors).

The functional parameters of the REClight device are as follows:

- Four analog input channels, dedicated to four different light sensors,
- Independent Conditioning of the analog signals in each channel,
- Digitizing of the four signals in a synchronous way, parallel in four analog to digital converters (ADCS),
- Sampling frequency: 500 Hz, ADC resolution: 16 bits,
- Real-time, digitally-controlled automatic gain control (AGC), independent in each channel,
- Integrated Real-time Clock for timestamps generation,
- Storage of the acquired data (with timestamps) in an internal FLASH memory,
- Access to the collected data via dedicated USB 2.0 port

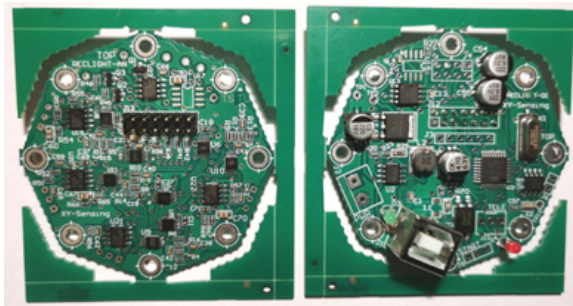


Figure 8 – Simplified block diagram of the REClight device.

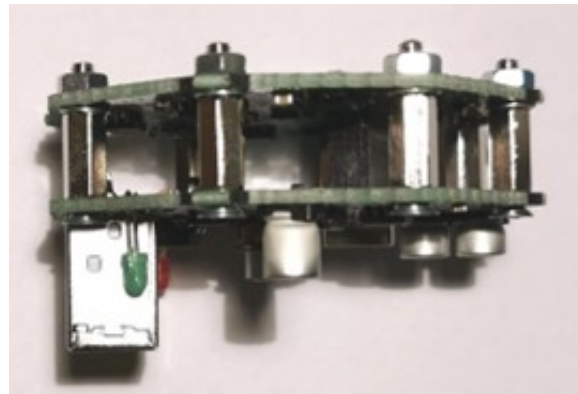


Figure 9 – Simplified block diagram of the REClight device.

- Separate serial port for telemetry connection with an external on-board computer,
- Dedicated digital input for external trigger signal,
- Power supply from one external source (typically: 2S or 3S Li-Ion battery, 7... 15 V DC).

### 3.3.2 Analog Processing Board

An internal architecture of the Analog Processing Board is presented in Fig. 10.

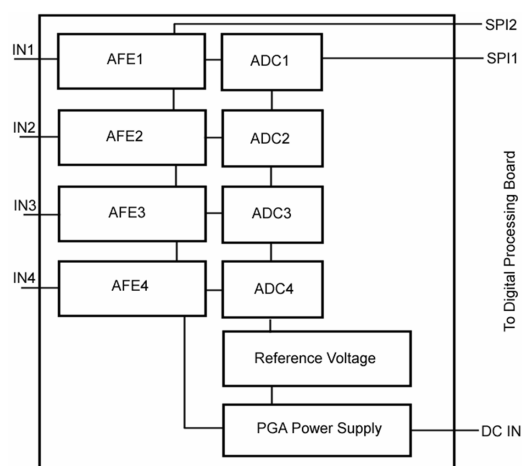


Figure 10 – Simplified block diagram of the REClight device.

The board contains four identical analog signal processing paths, each consisting of an Analog Front End (AFE) followed by an Analog to Digital Converter (ADC) and dedicated to a separate channel (or optoelectrical sensor). These circuits are supported by a dedicated source of a Reference Voltage ( $V_{ref} = 4.096 \text{ V}$ ), power supply filters and a special power supply circuit dedicated to Programmable Gain Amplifiers (PGAs) that should be powered with a voltage equal to the  $V_{ref}$  due to internal structure of their output stages. The general structure of the AFE implemented in each channel is

shown in Fig. 11.

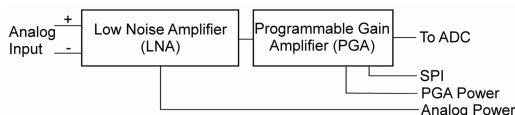


Figure 11 – Simplified block diagram of the REClight device.

The signal from the optoelectrical sensor is coupled in a differential way with a dedicated analog input of the device, and fed into a Low Noise Amplifier (LNA). The LNA is realized either as a transconductance amplifier (for photodiode sensors) or a non-inverting voltage amplifier (for IR thermopile sensor), since these sensors provide either current or voltage signal. In both cases, a special low-offset and low-noise Operational Amplifier (OpAmp) has been used, that can be powered asymmetrically with a low voltage (5 V DC). The transfer characteristics of LNA for photodiodes and IR thermopiles are plotted in Fig. 12, 13, respectively.

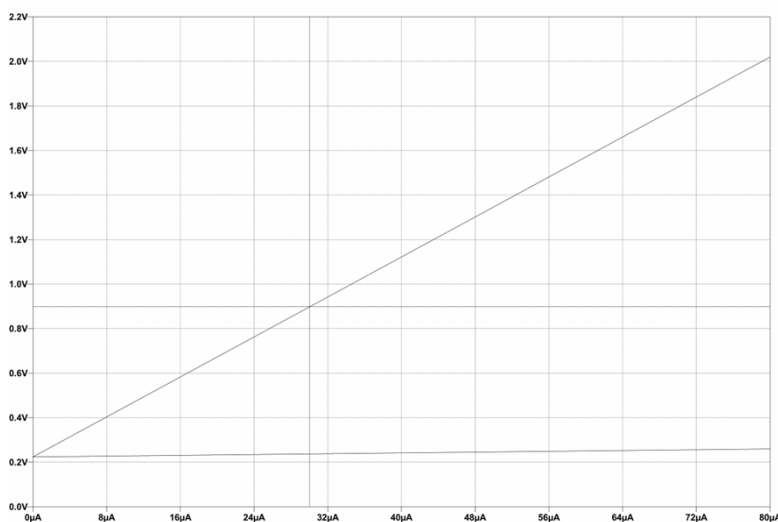


Figure 12 – Simplified block diagram of the REClight device.

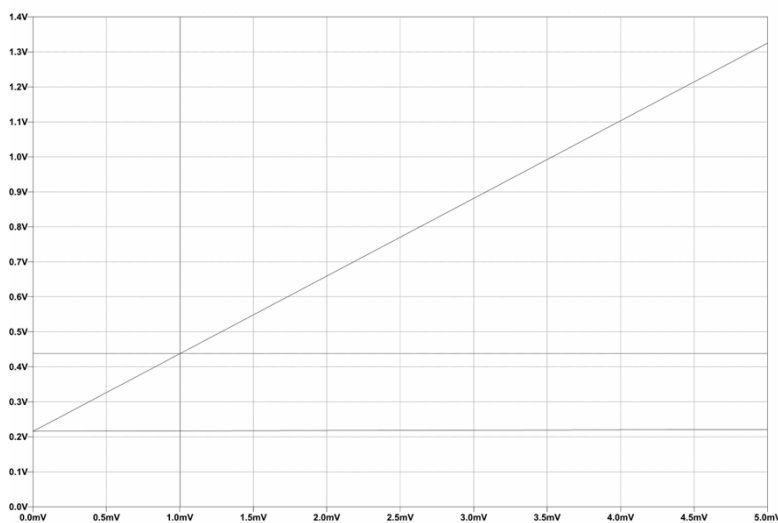


Figure 13 – Simplified block diagram of the REClight device.

The OpAmps in LNA stages are also designed to perform as an active low-pass filters at the same time, in order to suppress the high-frequency and noise components of the measured signals and

thus to avoid the aliasing effect in analog to digital conversion. A simulated frequency characteristic of the LNA designed for the IR thermopile sensor, operating as a voltage amplifier, is plotted in Fig. 14.

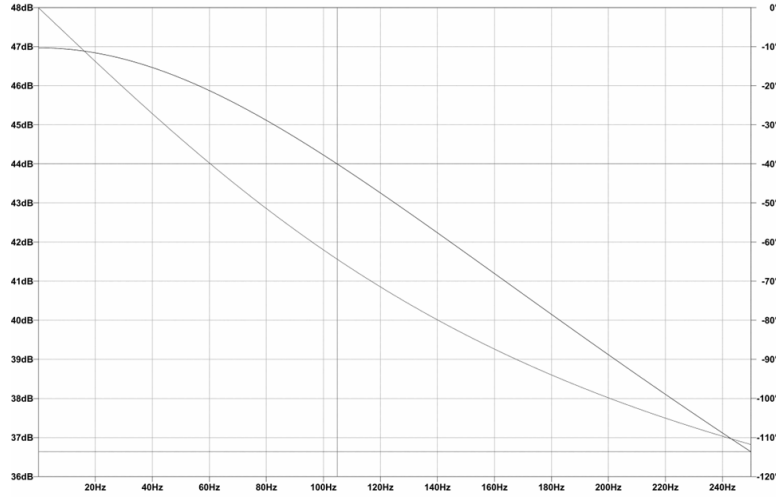


Figure 14 – Simplified block diagram of the REClight device.

The output voltage from the LNA is connected to the second-stage that performs a function of a Programmable-Gain Amplifier (PGA). The PGAs can be configured via common digital interface (Serial Peripheral Interface, SPI) to select one of the following voltage gain levels:

$$G_P \in \{0.2, 1, 0, 20, 30, 40, 60, 80, 120, 157\}, \quad (1)$$

independently for each channel. The actual gain level  $G_P$  can be either dynamically selected in Adaptive Gain Control algorithm that works in a real-time in the controlling software, or stay fixed according to a selection stored in the current configuration of the device. The voltage signal fed into the ADC, after passing the combined LNA (configured for photodiodes) and PGA, in a simplified form can be expressed as

$$U_{ADC} = I_S * G_{ILNA} * G_P + V_{REF}/2 \quad (2)$$

where  $I_S$  denotes the photodiode output current, and  $G_{ILNA}$  is the fixed current-voltage gain of the LNA. Similarly, the voltage provided to the ADC input from the analog channel configured for IR thermopile, after a few simplifications can be expressed as

$$U_{ADC} = U_S * G_{ULNA} * G_P + V_{REF}/2 \quad (3)$$

where  $U_S$  denotes the sensor output voltage, and  $G_{ULNA}$  is the fixed voltage gain of the LNA, implemented as a non-inverting OpAmp. Finally, the 16-bit integer value available at the ADC output that is stored in the FLASH memory as a measurement result is

$$W_{ADC} = [U_{ADC}/V_{REF}] * [2^{16} - 1] \quad (4)$$

where  $[*]$  is the floor function.

Each PGA output stage employs an additional OpAmp (embedded into the PGA chip) that is configured to act as an additional anti-aliasing lowpass filter.

### 3.3.3 Digital Processing board

A simplified block diagram of the Digital Processing Board is depicted in Fig. 15.

The main part of this board is an 8-bit RISC microcontroller (Microchip / Atmel ATmega 328P, known from the Arduino Nano evaluation modules), clocked with a crystal resonator (18.432 MHz). The first serial interface (SPI1), realized in a hardware, is connected to an external FLASH memory (for fast storing and reading of the acquired data) and to the control interface of PGAs in the Analog

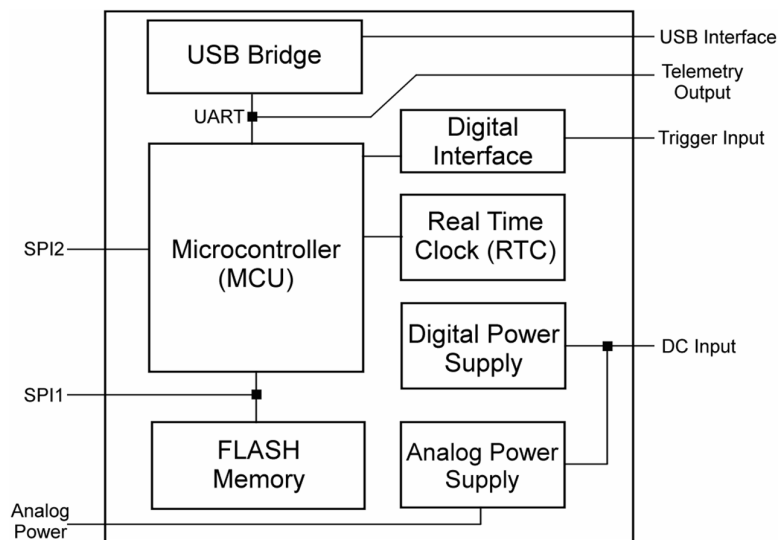


Figure 15 – Simplified block diagram of the REClight device.

Processing Board. The second SPI interface (SPI2) is realized in a MCU software and used to trigger ADCs and fetch their results after completing A/D conversion cycle. This interface is inactive for most of the time (especially during the A/D conversion) to reduce a noise level in the most sensitive parts of the device. The Real-Time Clock (RTC) is responsible for counting current date and time that is used for timestamping the measurement results during the data acquisition process. An asynchronous UART interface is used both for USB communication (via dedicated USB bridge) during device stand-by state, and for sending chunks of raw data in a real time to the Telemetry Output, during data acquisition state. This interface is configured for fast operation (460800 bit/s) to achieve a high data throughput. In the Digital Processing Board there is also a dedicated digital input interface (galvanically isolated from the rest of the circuit) that allows to send a trigger impulse (a voltage signal) to MCU to start the data acquisition process. A separate power supply circuits have been implemented for analog and digital parts to reduce the noise level in the Analog Processing Board and avoid digital signals crosstalk to the sensitive analog circuits. The entire device is powered from a single DC voltage provided typically from a small Li-Ion battery pack.

### 3.3.4 Operational principles

After power-up, the MCU performs internal reset and starts to execute the firmware that is stored in its internal FLASH memory. Firstly, the last-known configuration of the device is recalled from the internal nonvolatile EEPROM memory in the MCU so that once configured, only the DC power voltage and trigger signal need to be provided to the device to start another session of data acquisition. Secondly, the initialization of all the peripheral blocks is performed and then a self-test of the external FLASH memory, responsible for the measurement data storage. The contents of this memory is scanned to check the memory occupation level and to find the first address available for the storage. Such a procedure allows us to store several sessions of data acquisition, one after another, while each session can be terminated simply by power supply removal. The mentioned initial procedure of FLASH memory checking guarantees that previously recorded data cannot be overwritten. After completion of the mentioned power-up procedure, the MCU starts to monitor a state of the trigger input line. When an active state of this input is noticed for more than 100 ms, the data acquisition session is commenced. In this state, the ADC conversion results from all the measurement channels are periodically fetched and stored in the external FLASH memory, together with the current timestamps. If the automatic gain control (AGC) function is enabled, values of the samples are analyzed to detect peak values and dynamic range of the signal in each channel. During a programmed time intervals, the PGA gain setting can be modified upon the results of AGC algorithm, to avoid ADC saturation effect while making use of most of the ADC dynamic range at the same time. If the telemetry sending function is enabled, chunks of signal samples from all four channels can be also periodically sent via an UART interface connected with an external system (e.g., an on-board computer). Apart from the

trigger monitoring and performing data acquisition, the MCU can receive several commands from an UART interface. These commands are responsible for changing of the configuration, switching the operational modes of the device, as well as downloading measurement results stored in the external FLASH memory. The data acquisition session can be stopped with a proper command received from the UART, when the external FLASH occupancy reaches 100 percent level, or as a result of DC power loss. The capacity of this FLASH memory allows for storing up to 17 minutes of uninterrupted measurement results, which is more than enough to store data from an experimental flight onboard a small rocket.

### 3.4 Data obtained

The completion of the integration process of the system, along with the verification of its basic functionalities, has enabled the acquisition of the first results from measurements of variations in infrared radiation, visible light, and ultraviolet intensity. Ultimately, the goal is to develop a series of algorithms capable of precisely calculating the angular velocities of a rapidly rotating object based on the timing of intensity changes in various types of electromagnetic waves, which in reality reflect the object's rotations.

However, as a preliminary step, it is crucial to explain how the data obtained from individual sensors can contribute, in a broader context, to improving the accuracy of navigational data, particularly in situations where gyroscope saturation occurs due to conditions exceeding their measurement limits. Figure 16 below presents a general scheme for acquiring navigational data in the case of inertial navigation systems.

## System operation concept diagram

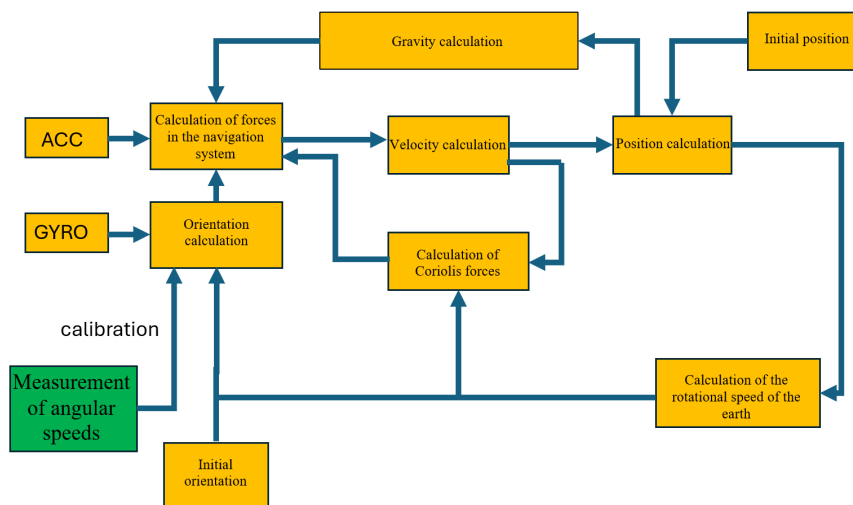


Figure 16 – System operation concept diagram.

As can be seen in the above diagram, the process of calculating navigational data in an inertial navigation unit is complex and multi-layered. In addition to feeding the navigation algorithms with sensor data, it also requires initial orientation and precise initial positioning. The system proposed in this scientific article allows for both the calibration of gyroscopes and the elimination of specific error components when measuring angular velocities within the measurement range, and the possibility of completely replacing gyroscopes with the sensors developed in this project when their measurement limits are exceeded.

Figure 17 below shows raw results obtained directly from the test setup during measurements conducted on a cloudy afternoon (the graph shows the obtained signal, which is the voltage value expressed in millivolts generated as a function of time). The first test case involved running the setup at angular velocities of 360, 720, 1080, and 1440 °/s for six angles of attack ranging from 0 to 50 °(with 10° increments starting from zero). Furthermore, to accurately determine the values of the data obtained from the sensors, it was assumed that each of the four angular velocities would be

maintained for 6 seconds at each angle on the test setup, and then, after reaching the maximum angle of attack, i.e.,  $50^\circ$ , the setup would switch to the next angular velocity. The tests started with an angular velocity of 360 %/s and an angle of attack of  $0^\circ$  relative to the level of the ground on which the setup was positioned.

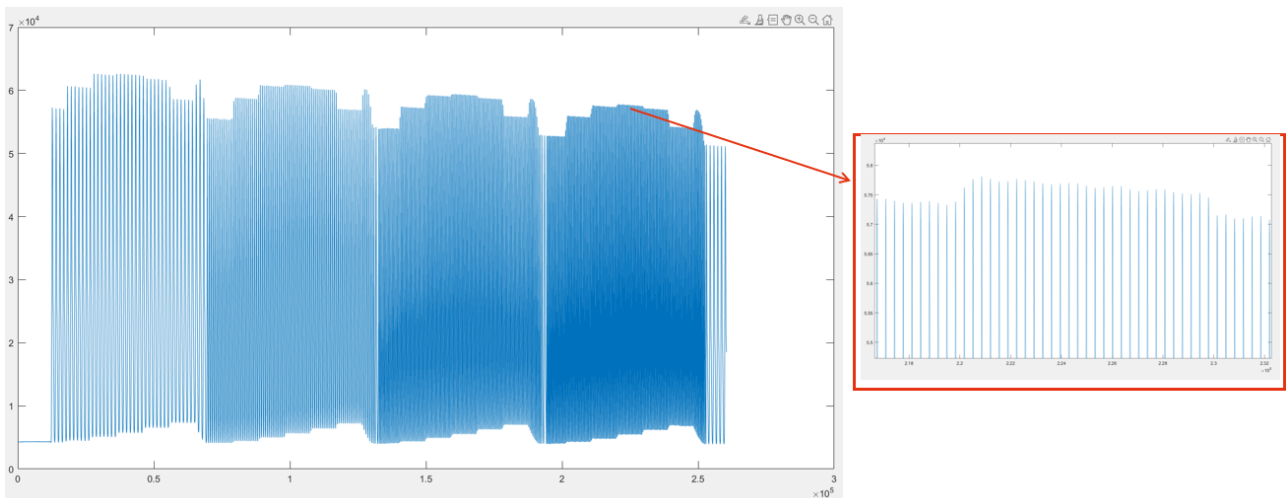


Figure 17 – The obtained measurement results for the VTB1013 Excelitas sensor.

When analyzing the obtained results, it is important to first highlight that the recorded signal has a continuous nature, with no distortions or noise in the visible and near infrared light sensor intensity from the VTB1013 Excelitas sensor. Moreover, the obtained signal characteristics clearly indicate the presence of strong signal maxima and minima, which correspond respectively to the heated surface of the Earth and the low temperature of the sky. Furthermore, it should be noted that the observable changes in the recorded maximum and minimum signal values are due to the change in the angle of attack of the head with the infrared sensor, which has an angular range of only a few degrees. However, the change in the sensor's angle of attack relative to the Earth did not affect the signal pattern in any way. Based on these results, it was also determined that the signal's nature does not depend on the angular velocity for each of the tested angular velocities, namely: 360, 720, 1080, 1440 %/s.

In the next step, it was decided to preliminarily verify the validity of the concept presented above by examining the nature of the obtained signal for 4 sensors covering all planned spectral ranges of radiation, including visible light, infrared, and ultraviolet radiation. In particular, the study was conducted for the following sensors:

- CH1 (Vis) - visible light ultraviolet radiation sensor GVBL-T14GD,
- CH2 (Vis) - visible and near infrared light sensor VTB 1013H,
- CH3 (UV) - ultraviolet radiation sensor GUVA-T21GD-U,
- CH4 (IR) - Infrared sensor HMS M11 L3.0F8.0,

For this purpose, tests were conducted to achieve a linearly increasing angular velocity in the range of 0-3600 %/sec for a zero angle of attack of the test stand. The tests were carried out under conditions of strong daytime sunlight and during a cloudy night. The obtained data, which are a function of the voltage from the sensors expressed in millivolts per unit of time expressed in seconds, are presented in the form of graphs.

Figure 18 shows the data obtained for cloudless sky conditions with strong sunshine occurring at noon.

Figure 19 shows the results obtained for cloudy night conditions.

The obtained data demonstrate the presence of pronounced extrema in the function for sensors CH1, CH2, and CH3 under daytime conditions, while only a noisy signal was observed under the same conditions for sensor CH4. In contrast, under nighttime conditions, an entirely opposite trend was observed, with a noisy signal from sensors CH1, CH2, and CH3, while a very clear signal exhibiting pronounced extrema in the function was obtained from sensor CH4.

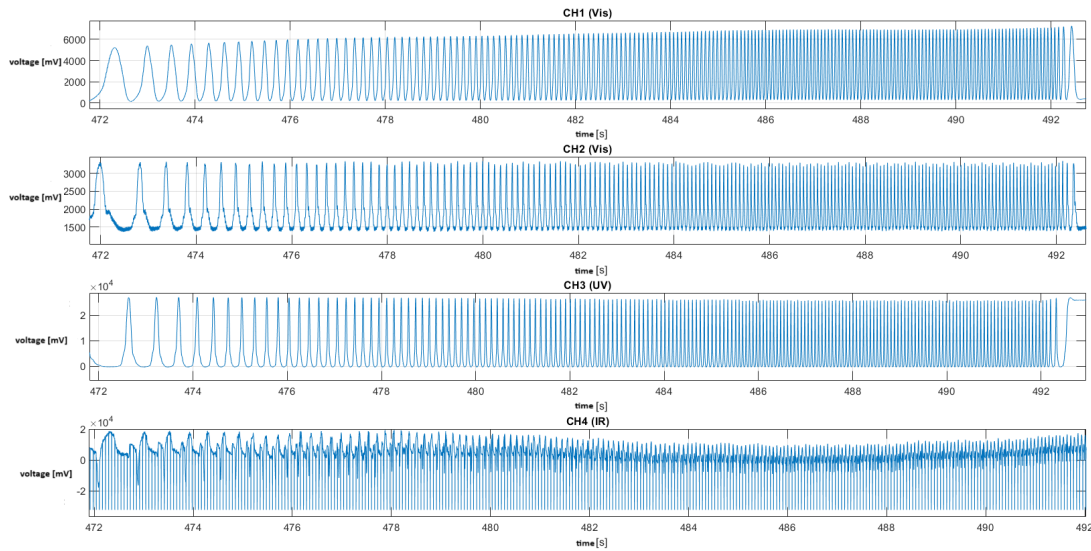


Figure 18 – The obtained measurement results for the all sensors - conditions of clear sky and high sunshine at noon.

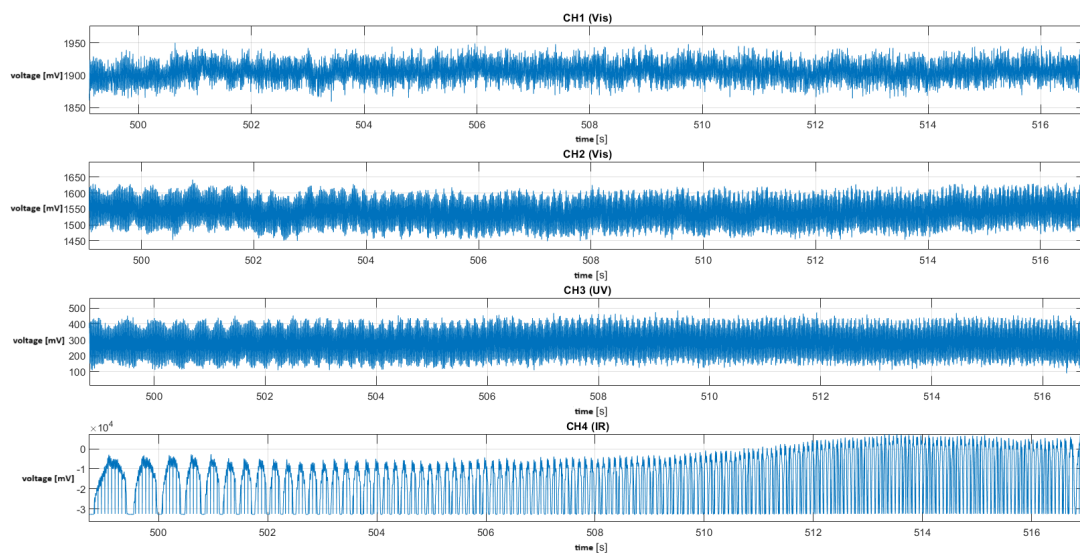


Figure 19 – The obtained measurement results for the all sensors - midnight cloudy conditions.

#### 4. Conclusions

In conclusion, it should be emphasized that all planned tasks were completed. Specifically, based on the conducted literature review presenting the current state of knowledge, a research problem was identified. It involved the need to develop a reference system for acquiring navigational data in the rotation channel using an interference-resistant measurement method.

To address the defined research problem, a technology was proposed based on various sensors of electromagnetic wave radiation (measuring radiation intensity), starting from infrared waves (ranging from 780 nanometers to 1 millimeter), visible light (wavelengths from 380 to 750 nanometers), ultra-violet radiation in the UV-A range (from 320 to 400 nanometers), and a combination of the aforementioned electromagnetic waves in the form of an integrated single sensor. Furthermore, to investigate the potential for implementing the technology, a dedicated test setup was designed, manufactured, and tested. The activation process confirmed all the assumed functionalities of the test stand.

Based on the obtained results from the VTB1013 Excelitas visible and near infrared light sensor for six angles of attack, ranging from 0 to 50° (with 10° increments starting from zero), and four angular velocities of 360, 720, 1080, and 1440 %/s, it was unequivocally determined that the obtained signal characteristics allow for precise determination of the angular velocities of a fast-rotating object.

In the test aimed at evaluating the feasibility of using 4 sensors operating with different types of radiation under conditions of strong daytime sunlight and a cloudy night, it was demonstrated that employing diverse sensors is essential. It is also worth emphasizing that sensors based on electromagnetic radiation directly from the Sun, within the angular velocity range of 0-3600 %/s, exhibited signal characteristics that enabled the identification of pronounced extrema and function minima. In contrast, the example of a cloudy night revealed that only the sensor utilizing infrared radiation and measuring the intensity of infrared radiation from the Earth's atmosphere and surface, within the same angular velocity range, provided signal characteristics containing pronounced extrema and minima. For further development of the proposed technology, it is necessary to conduct a detailed process of testing and research under varied atmospheric conditions. In particular, it is essential to gather measurement results from sensors recording all types of electromagnetic radiation (infrared, visible light, ultraviolet) in such atmospheric conditions as: cloudy winter days and nights, stormy spring periods, sunny summer days and clear summer nights, foggy autumn mornings and nights, as well as other typical weather conditions in Central and Eastern Europe. Conducting detailed tests and research under diverse atmospheric conditions will enable the construction of a dedicated database that will allow for the correct development of algorithms for estimating navigational data, especially navigational data in the rotation channel. The research should be conducted for several scenarios, including changes in the angle of attack within the range of 0-50° and changes in angular velocities achieved on the measuring head for values of at least 0-3600 %/s.

### 5. Copyright Issues

The copyright statement is included in the template and must appear in your final pdf document in the position, style and font size shown below. If you do not include this in your paper, READ is not allowed and will not publish it.

### 6. Contact Author Email Address

The contact author email address should appear explicitly in this section to facilitate future contacts. For example [mailto: dawid.florczak@pw.edu.pl](mailto:dawid.florczak@pw.edu.pl)

### 7. Copyright Statement

The authors confirm that they, and/or their company or organization, hold copyright on all of the original material included in this paper. The authors also confirm that they have obtained permission, from the copyright holder of any third party material included in this paper, to publish it as part of their paper. The authors confirm that they give permission, or have obtained permission from the copyright holder of this paper, for the publication and distribution of this paper as part of the READ proceedings or as individual off-prints from the proceedings.

### References

- [1] Wang, Jie Xuan, and Xin Ming Qian. "Application and Development of MEMS in the Field of Aerospace." *Applied Mechanics and Materials*. Trans Tech Publications, Ltd., September 2014. <https://doi.org/10.4028/www.scientific.net/amm.643.72>.
- [2] Yuan, Xiaoqiao, Jie Li, Xi Zhang, Kaiqiang Feng, Xiaokai Wei, Debiao Zhang, and Jing Mi. 2021. "A Low-Cost MEMS Missile-Borne Compound Rotation Modulation Scheme" *Sensors* 21, no. 14: 4910. <https://doi.org/10.3390/s21144910>
- [3] Gill, Waqas Amin, Ian Howard, Ilyas Mazhar, and Kristoffer McKee. 2022. "A Review of MEMS Vibrating Gyroscopes and Their Reliability Issues in Harsh Environments" *Sensors* 22, no. 19: 7405. <https://doi.org/10.3390/s22197405>
- [4] Chiang, Kai-Wei, Thanh Trung Duong, Jhen-Kai Liao, Ying-Chih Lai, Chin-Chia Chang, Jia-Ming Cai, and Shih-Ching Huang. 2012. "On-Line Smoothing for an Integrated Navigation System with Low-Cost MEMS Inertial Sensors" *Sensors* 12, no. 12: 17372-17389. <https://doi.org/10.3390/s121217372>

- [5] Yang, Qinghua, Yang Shen, Xuetao Sun, and Changfa Wang. 2024. "A Novel Method and System Implementation for Precise Estimation of Single-Axis Rotational Angles" *Sensors* 24, no. 17: 5795. <https://doi.org/10.3390/s24175795>
- [6] Bancroft, Jared B., and Gérard Lachapelle. 2011. "Data Fusion Algorithms for Multiple Inertial Measurement Units" *Sensors* 11, no. 7: 6771-6798. <https://doi.org/10.3390/s110706771>
- [7] Pachwicewicz, M., Weremczuk, J. "Accuracy estimation of the sounding rocket navigation system." In: 2018 XV International Scientific Conference on Optoelectronic and Electronic Sensors (COE), pp. 1–4 (2018). <https://doi.org/10.1109/COE.2018.8435180>
- [8] Ünsal Öztürk, Derya, and Aydan M. Erkmén. 2022. "Coriolis Vibratory MEMS Gyro Drive Axis Control with Proxy-Based Sliding Mode Controller" *Micromachines* 13, no. 3: 446. <https://doi.org/10.3390/mi13030446>
- [9] S.M. Dildar Ali, U. Iqbal Bhatti, K. Munawwar, U. Al-Saggaf, Shoaib Mansoor, Jamshaid Ali, "Gyroscopic drift compensation by using low cost sensors for improved attitude determination", *Measurement*, Volume 116, 2018, Pages 199-206, ISSN 0263-2241, <https://doi.org/10.1016/j.measurement.2017.11.003>.
- [10] Goraj, Z.J. and Cichocka, E. (2016), "Influence of weak and strong gyroscopic effects on light aircraft dynamics", *Aircraft Engineering and Aerospace Technology*, Vol. 88 No. 5, pp. 613-622. <https://doi.org/10.1108/AEAT-03-2015-0076>
- [11] El-Sheimy, N., Youssef, A. Inertial sensors technologies for navigation applications: state of the art and future trends. *Satell Navig* 1, 2 (2020). <https://doi.org/10.1186/s43020-019-0001-5>
- [12] Zhao, Yuan, Xuguang Yue, Fusheng Chen, and Chen Huang. "Extension of the Rotation-Rate Measurement Range with No Sensitivity Loss in a Cold-Atom Gyroscope." *Physical Review A* 104, no. 1 (July 2021): 013312. <https://doi.org/10.1103/PhysRevA.104.013312>.
- [13] Liu, Zhi, and Gang Han. "Resonant MEMS Accelerometer with Low Cross-Axis Sensitivity—Optimized Based on BP and NSGA-II Algorithms." *Micromachines* 15, no. 8 (2024): 1049. <https://doi.org/10.3390/mi15081049>.
- [14] Ru, Xu, Nian Gu, Hang Shang, and Heng Zhang. MEMS Inertial Sensor Calibration Technology: Current Status and Future Trends. *Micromachines* 13, no. 6 (2022): 879. <https://doi.org/10.3390/mi13060879>.
- [15] Ackerman, Robert K. "Russian Electronic Warfare Targets NATO Assets." *AFCEA International*, November 1, 2017. <https://www.afcea.org>.